Cell. Mol. Life Sci. (2017) 74:2689–2707
DOI 10.1007/s00018-017-2495-z

Cellular and Molecular Life Sciences

ORIGINAL ARTICLE

Kinetic analysis, size profiling, and bioenergetic association of DNA released by selected cell lines in vitro

Janine Aucamp[1] · Abel J. Bronkhorst[1] · Dimetrie L. Peters[1] · Hayley C. Van Dyk[1] · Francois H. Van der Westhuizen[1] · Piet J. Pretorius[1]

Received: 15 November 2016 / Revised: 19 February 2017 / Accepted: 22 February 2017 / Published online: 18 March 2017

Abstract Although circulating DNA (cirDNA) analysis shows great promise as a screening tool for a wide range of pathologies, numerous stumbling blocks hinder the rapid translation of research to clinical practice. This is related directly to the inherent complexity of the in vivo setting, wherein the influence of complex systems of interconnected cellular responses and putative DNA sources creates a seemingly arbitrary representation of the quantitative and qualitative properties of the cirDNA in the blood of any individual. Therefore, to evaluate the potential of in vitro cell cultures to circumvent the difficulties encountered in in vivo investigations, the purpose of this work was to elucidate the characteristics of the DNA released [cell-free DNA (cfDNA)] by eight different cell lines. This revealed three different forms of cfDNA release patterns and the presence of nucleosomal fragments as well as actively released forms of DNA, which are not only consistently observed in every tested cell line, but also in plasma samples. Correlations between cfDNA release and cellular origin, growth rate, and cancer status were also investigated by screening and comparing bioenergetics flux parameters. These results show statistically significant correlations between cfDNA levels and glycolysis, while no correlations between cfDNA levels and oxidative phosphorylation were observed. Furthermore, several correlations between growth rate, cancer status, and dependency on aerobic glycolysis were observed. Cell cultures can, therefore, successfully serve as closed-circuit models to either replace or be used in conjunction with biofluid samples, which will enable sharper focus on specific cell types or DNA origins.

Keywords Cell cultures · Circulating DNA · Cell-free DNA · Bioenergetics flux parameters · Aerobic glycolysis

Introduction

Since the discovery of circulating DNA (cirDNA) in human plasma [1], multiple studies have reported elevated levels of cirDNA in patients with various ailments, especially cancer (reviewed in [2]). In addition, the discovery of cell-free fetal DNA in maternal plasma has opened new avenues for the development of non-invasive prenatal screening methods [3]. However, despite more than 40 years of research, only one clinically validated application of cirDNA analysis as a disease screening marker is currently available, namely the Cobas® EGFR Mutation Test v2 (Roche Molecular Systems) for predicting the response of non-small cell lung cancers to treatment, particularly erlotinib (a tyrosine kinase inhibitor also known as Tarceva) [4, 5]. Although the development of clinical tests has been delayed by technological limitations and associated costs, this is becoming less of an excuse considering the continual and rapid improvements in sample handling products and high-throughput/ultra-sensitive techniques (e.g. NGS and ddPCR), which, in turn, reduce processing costs (discussed in [5]).

The lack of clinical applications for cirDNA analysis can be explained by the shortage of standard operating procedures and assay validation, which prevent the identification of normal reference values for correlating with diseases or the establishment of cut-off values for diagnosis and prognosis. This major drawback has been acknowledged by

✉ Janine Aucamp
aucampj@telkomsa.net

[1] Human Metabolomics, North-West University, Hoffman Street, Potchefstroom 2520, South Africa

several researchers [5–12]. Furthermore, our knowledge regarding the biological properties, origin, and function of cirDNA is still lacking considerably.

Thierry et al. [13] has recently demonstrated the heterogeneity of the cirDNA population in plasma samples by highlighting various potential sources from which DNA could be released into circulation. It has also recently been demonstrated that the cirDNA derived from one cell or tissue type can be a product of different time dependent and environmentally modulated release mechanisms, which results in the presence of different amounts of cirDNA in a sample at a given time [14]. Research by Mittra et al. [15] showed potential damaging effects of apoptosis-derived cirDNA on cells, but also observed differences between the effects of cirDNA extracted from cancer patients and healthy controls, which may imply that the origin of the cirDNA may affect its function or effect on adjacent tissues once released into circulation. In addition, other researchers have demonstrated that the cellular release of mitochondrial DNA fragments can cause an inflammatory response [16–18]. However, analysis of these different effects in in vivo samples may prove to be difficult due to the presence of a vast range of putative cirDNA sources [19].

To overcome this problem, the implementation of in vitro cell culture models to study the biological properties of cirDNA has been proposed [14]. The purpose of this paper is to further encourage the utilization of cell cultures in elucidating the origin, composition, and function of cirDNA. Our previous studies have shown that the DNA released by cultured osteosarcoma cells into the growth medium [cell-free DNA (cfDNA)] consists of varying ratios of both apoptotic and actively released DNA fragments at various time intervals of incubation [14]. Furthermore, the DNA size profile observed in this study was shown to bear great similarity with the size profile of cirDNA derived from human blood, which exemplifies the potential of in vitro studies to aid in vivo research regarding the biological properties of cfDNA.

Under normal conditions, cells synthesize ATP most efficiently through glycolysis and oxidative phosphorylation (OXPHOS). Many cancers, however, undergo a metabolic conversion referred to as the 'glycolytic switch', after which glycolysis becomes uncoupled from respiration and lactic acid fermentation is used as the primary process for ATP production instead [20]. Such a switch occurs normally as a rescue mechanism for the production of energy during hypoxic conditions. In some cancer cells, however, the cells develop a particular glycolytic phenotype described by the controversial Warburg hypothesis as 'aerobic glycolysis'. At the first glance, it may seem like a highly inefficient path of energy production that converts far less ADP to ATP than OXPHOS. The benefits of this metabolic conversion, however, is that it potentially enables rapid ATP production and provides carbon intermediates allocable to branched biosynthetic pathways, which allows increased biomass expansion. Supporting this notion, the most common mutations in human tumors include mutations of the signalling pathways that regulate cellular biosynthesis and aerobic glycolysis [21]. Cancer cell metabolism is devoted primarily to consume glucose and glutamine, with very little glucose being used for OXPHOS [22–24] and correlations have been found between aerobic glycolysis and cancer cell proliferation [20]. It has also been determined that a switch of cancer cell metabolism from glycolysis to OXPHOS, upon inhibition of the pentose phosphate pathway, results in decreased proliferation [20]. The utilization of these unique metabolomic profiles of cancers as therapeutic targets may yield very promising new therapies [22, 25, 26]. Moreover, focusing on these characteristics may provide more insight into the elucidation of the biochemical characteristics and biological functions of cirDNA.

Therefore, in this study, we first compared the release patterns and fragment sizes of the cfDNA derived from various cell lines to determine whether variations in tissue origin, growth rate, and cancer status can influence cfDNA release characteristics. These cfDNA levels were then compared to the bioenergetics flux parameters, OXPHOS and glycolysis, of the respective cell lines to determine whether or not cfDNA release is affected by or dependent on cellular metabolic activity.

Materials and methods

Cell cultures and growth conditions

For the purpose of this study, the following seven cell lines with varying tissue origins, growth rate, and cancer status were identified: (1) rhabdomyosarcoma (RD) (ATCC® CCL-136™), large malignant tumor cells with a slow growth rate; (2) skin fibroblast (FIBRO) {also referred to as ZANLP in our previous study (Bronkhorst et al. [14])}, normal or healthy skin cells with a slow growth rate; (3) melanoma (A375) (ATCC® CRL-1619™), malignant skin cancer cells with a fast growth rate; (4) keratinocytes (HaCat) (AddexBio), spontaneously immortalized human skin cells with a relatively fast growth rate; (5) cervical adenocarcinoma (HeLa) (ATCC® CCL-2™), human papilloma virus (HPV)-induced cancer cervix epithelial cancer cells; (6) human embryonic kidney (HEK-293) (ATCC® CRL-1573™), normal or healthy adenovirus-transformed embryonal kidney cells; (7) hepatocellular carcinoma (HepG2) (ATCC® HB-8065™), cancerous liver epithelial cells with a significantly slow growth rate when cultured in Roswell Park Memorial Institute (RPMI) 1640 medium.

As an eighth cell line, data from our previous research regarding osteosarcoma (143B) (ATCC® CRL-8303™), bone cancer cells with a fast growth rate [14], were also added for comparison.

RD and FIBRO cells were grown in Dulbecco's modified Eagle's medium (Hyclone DMEM/high glucose), containing 4 mM L-glutamine, 4500 mg/L glucose, and 1 mM sodium pyruvate (Thermo Scientific), fortified with 10% fetal bovine serum (FBS) (Biochrom) and 1% penicillin streptomycin (Lonza). A375, HeLa, HaCaT, and HEK-293 cells were grown in the same growth medium with additional supplementation of 1% L-glutamine (Lonza), 1% non-essential amino acids (Lonza) and 1% amphotericin B (Biochrom). HepG2 was grown in RPMI 1640 (Hyclone), containing 2.05 mM L-glutamine (Thermo Scientific), fortified with 10% FBS, 1% penicillin streptomycin, and 1% amphotericin B. Initially, all of the cell lines were grown in 175 cm^2 flasks (Corning) to 90–100% confluence and incubated in a humidified atmosphere at 37 °C and 5% CO_2. Once the cell cultures reached the desired confluence, the cells were detached from the flasks via trypsinization and seeded into 75 cm^2 flasks (Corning) as follows: (1) the HaCaT and A375 cells at 30% confluence; (2) the RD, FIBRO, and HepG2 cells at 50% confluence; and (3) the, HeLa and HEK-293 cells at 25% confluence. Ten 75 cm^2 flasks were prepared for FIBRO cells, eighteen 75 cm^2 flasks for HaCaT cells, and twelve 75 cm^2 flasks for the remaining cell lines. All of the flasks contained a final volume of 12 mL. The 75 cm^2 flasks were incubated for 12 h, after which the growth medium was replenished. After this time, pairs of flasks were incubated for different time intervals for each cell line. The flask pairs of the A375 and RD cells were incubated for 4, 8, 12, 16, 20, and 24 h. The flask pairs of the HepG2, HeLa and HEK-293 cells were incubated for 4, 8, 12, 24, 48, and 72 h. The flask pairs of the HaCaT cells were incubated for 0, 2, 4, 6, 8, 12, 24, 36, and 48 h. The flask pairs of the FIBRO cells were incubated for 4, 18, 44, 72, and 98 h. The last time interval of each cell line serves as the time interval after which the cell lines reached confluence.

Sample collection and processing

At the end of incubation, the growth medium was collected in 15 mL tubes (SPL) and then centrifuged at 5000×*g* for 10 min and transferred to fresh 15 mL tubes. The samples were then stored at −80 °C until use. The cells were collected by trypsinization in 15 mL tubes, centrifuged at 5000×*g* for 5 min, rinsed with PBS, pelleted at 5000×*g* for 5 min, and stored at −80 °C for the extraction and determination of total cellular protein content.

Extraction and quantification of cellular protein

The frozen cell pellets were suspended in 3–4 mL cold PBS and 500 µL samples aliquots were sonicated with the Bioruptor UCD-200 (Diagenode). Before usage, the Bioruptor was cooled to 4 °C using distilled water and ice. Sonication settings were: power, H-position (high); sonication cycle, 30 s on/30 s off; total sonication time, 5–10 cycles. The total cellular protein content was quantified with the Qubit® Protein Assay kit and Qubit® 2.0 Fluorometer (Invitrogen, Life Technologies) according to the manufacturer's instructions.

Extraction and quantification of cell-free DNA

CfDNA was extracted directly from the growth medium using the NucleoSpin Gel and PCR Clean-up kit (Macherey-Nagel, Düren, Germany) according to the manufacturer's PCR clean-up instructions. Samples were thawed at 37 °C in a temperature controlled water bath, vortexed, and centrifuged briefly, and cfDNA was extracted in triplicate for each biological replicate. Extraction samples were prepared by mixing growth medium in a ratio of 1:2 with binding buffer NTI. The individual samples were vortexed, centrifuged briefly, the entire volume added to spin columns in three 600 µL regiments, and centrifuged at 11,000×*g* for 1 min at room temperature. The columns were then washed twice with wash buffer and the cfDNA eluted into 20 µL of elution buffer. To collect sufficient amounts of cfDNA for DNA fragment analysis, bulk extraction of the cfDNA of HEK-293 samples was performed using the NucleoSpin Gel and PCR Clean-up kit according to the manufacturer's PCR clean-up instructions, except binding buffer NTB was used instead of NTI. The cfDNA of each sample was quantified with the Qubit® dsDNA High Sensitivity Assay kit and Qubit® 2.0 Fluorometer (Invitrogen, Life Technologies) according to the manufacturer's instructions.

Fragment size evaluation of cell-free DNA

Capillary electrophoresis (CE) was performed to analyse the size distribution of the cfDNA that was extracted at the different time intervals for each cell line. The microchips and reagents of the High Sensitivity DNA kit were used according to the manufacturer's instructions and analyses performed using the Agilent 2100 Bioanalyzer (Agilent Technologies Inc., Santa Clara, CA) equipped with Expert 2100 software. Nucleic acids are separated analogously to CE, normalized to a ladder and two DNA markers, of which the sizes are calculated automatically by the software. The final results are displayed as electropherograms, where the two major peaks present at 35 and 10,380 bp in each electropherogram represent the two

size markers used to calculate the size of unknown samples and deviations from the baseline indicate the sizes of the cfDNA present in the samples.

Bioenergetic analyses

To assess the cellular metabolic activity for each of the eight cell lines, the Seahorse XFe96 Extracellular Flux analyser (Seahorse Biosciences, USA) was used. This instrument is capable of simultaneously measuring, in real-time, the oxygen consumption rate (OCR) and extracellular acidification rate (ECAR) of cells, representatives of the OXPHOS and glycolytic activity, respectively. Two different tests were carried out according to the manufacturer's instructions, namely the Seahorse XF Cell Mito Stress Test Kit and Seahorse XF Glycolysis Stress Test Kit (Seahorse Biosciences, USA) under similar conditions to that described by Zandberg et al. [27]. For both analyses, all cell lines were seeded at a range of cell seeding densities after which the final cell seeding density of 10,000 cells/well, with 5–6 replicate wells ($n = 5–6$), was selected, since all cell lines provided satisfactory results (cells were not over-confluent and provided OCR and ECAR readings within the acceptable ranges set out by the manufacturer) at this density. After seeding, all cells were incubated for 23 h under the conditions described in "Cell cultures and growth conditions". Thereafter, the growth media were replaced with assay media (modified DMEM supplemented with 2 mM L-glutamine, pH 7.4) for both tests (with the additional supplementation of 1 mM pyruvate and 5 mM glucose for the Mito Stress Test) and incubated for 1 h in a non-CO_2 incubator.

The instrument protocol consisted of three measurement cycles (3 min mix and 3 min measure per cycle) at the start of the analysis as well as following each of the three compound injections. For the Mito Stress Test, the following compounds were injected: 1 µM oligomycin (ATP synthase inhibitor), 0.5–0.75 µM FCCP (an uncoupler injected at the optimal concentration per cell line) and finally 0.5 µM rotenone (complex I inhibitor) and antimycin A (complex III inhibitor). The Glycolysis Stress Test included the following injections: 10 mM glucose, 1 µM oligomycin, and 50 mM 2-deoxyglucose (a glucose analogue). To account for differences in the proliferation rates of different cell lines and thus differences in cell seeding densities at the time of the XF analysis, all cells were normalized against total DNA content using the CyQUANT Cell Proliferation Assay Kit (Life Technologies, USA) according to the manufacturer's instructions. Version 2.2 of the Seahorse Wave software was used to process and analyse all results, while all outliers were removed using the Tukey method [28].

Statistics

All statistical analyses were performed and all graphs constructed using GraphPad Prism 7 (Version 7.0.2). The bioenergetic results were correlated to cfDNA release using Pearson's correlation coefficient (r), where a p value of less than 0.05 indicated a statistically significant result.

Results and discussion

In this study, the cfDNA release patterns and fragment size distributions of multiple cell lines were elucidated to determine whether or not variations in tissue origin, growth rate, and cancer status can influence cfDNA release characteristics. The bioenergetics flux parameters, OXPHOS and glycolysis, of each cell line were also determined and correlations between the metabolic activity and the cfDNA release levels of the cell lines evaluated.

Cell-free DNA release patterns

The release of cfDNA by eight cell lines after growth medium renewal was characterized over time. Figure 1 shows the cfDNA release levels quantified for each cell line, whereas Fig. 2 presents the cfDNA yields normalized to the total cellular protein of the cells collected from the flasks at each time interval. All of the cell lines were grown to confluence, after which the experimental sampling was terminated. Three distinct cfDNA release patterns were detected over time during the exponential growth phase of the cell lines (Fig. 2): (1) HepG2 and 143B cells showed a tendency of increasing cfDNA levels, (2) HeLa, RD and HEK-293 showed a tendency of decreasing cfDNA levels, and (3) the skin cells HaCaT, FIBRO, and A375 showed varied levels of increasing and decreasing cfDNA release with significant standard deviations.

HepG2 cells showed significantly high levels of cfDNA release [nearly 1.2 ng/µg protein (Fig. 2b)], with an increase in cfDNA release (ng per flask) over time, reaching its highest level at 48 h, followed by a significant decrease at 72 h (Fig. 1a). The large amount of cfDNA from the HepG2 cells is theorized to occur due to the prolonged exposure (48 h) of a relatively large amount of slow growing cells (seeded at 50% confluence). The cells also had a tendency to clump together rather than forming a monolayer, which may indicate that the cells could have reached confluency earlier than visually predicted. In a separate experiment, the growth medium of the HepG2 cells was changed from RPMI to high glucose DMEM fortified with non-essential amino acids and L-glutamine, resulting in a significant increase in cell growth rate (requires seeding at 15% confluence for cells to reach confluence within 72 h), no cell

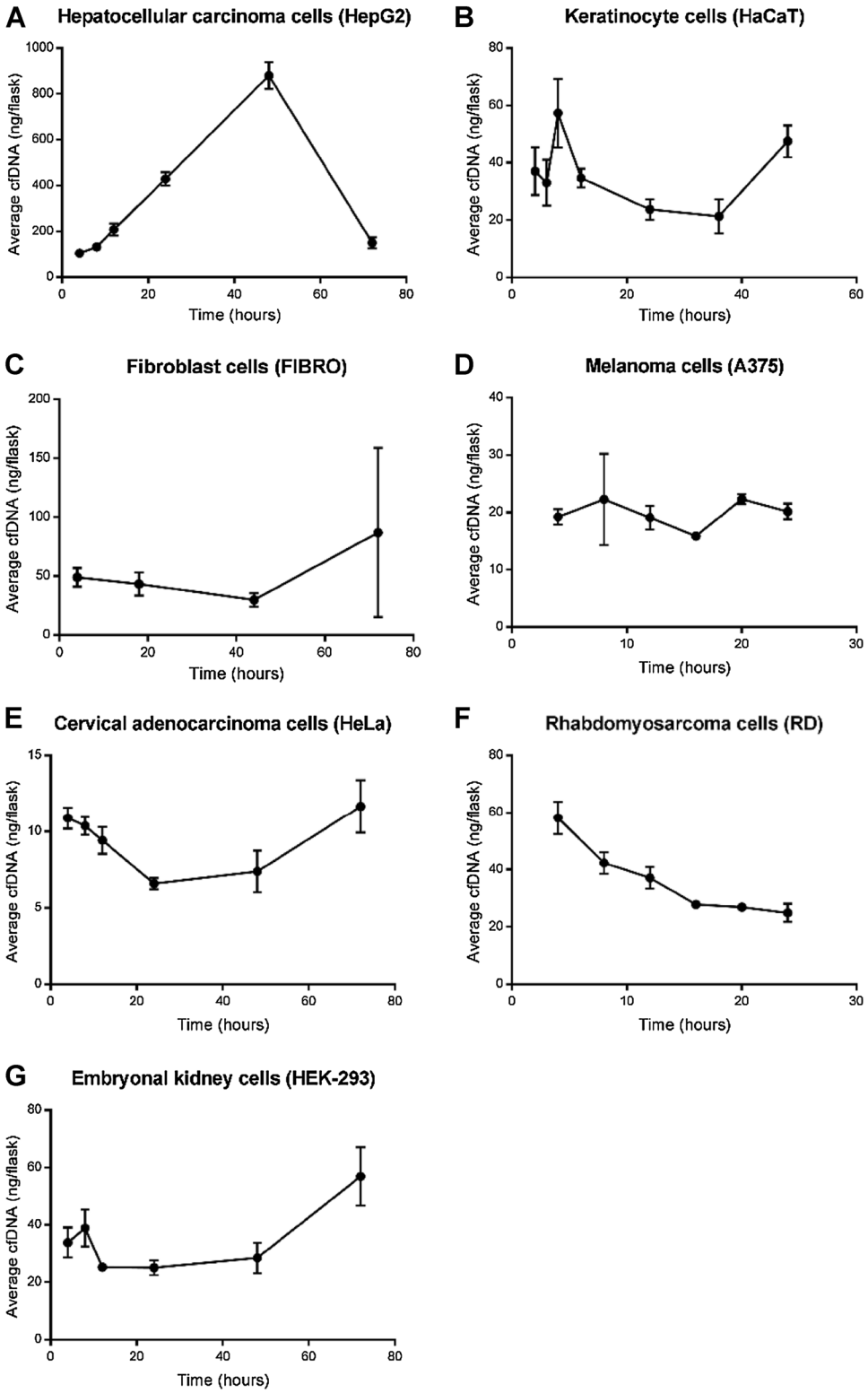

Fig. 1 CfDNA levels (ng/flask) of **a** HepG2, **b** HaCaT, **c**FIBRO, **d** A375, **e** HeLa, **f** RD, and **g** HEK-293 cell lines after several time intervals of incubation following medium renewal. The value of each bar represents the average (±SD, $n=6$) amount of cfDNA released in 12 mL of growth medium at each time interval

clumping, and a significant decrease in cfDNA release levels (30 pg/µg protein at 48 h).

Comparison of our previous results of 143B cells [14] (Fig. 2a) with HepG2 cells (Fig. 2b) revealed a similar cfDNA release pattern (pg/µg protein) with a gradual increase in cfDNA levels, followed by a significant decrease as the cell confluence increased. The significant decrease in cfDNA level of HepG2 and 143B cells at 72 and 28 h, respectively, was likely due to degradation via extracellular DNases. Studies have shown that healthy subjects present

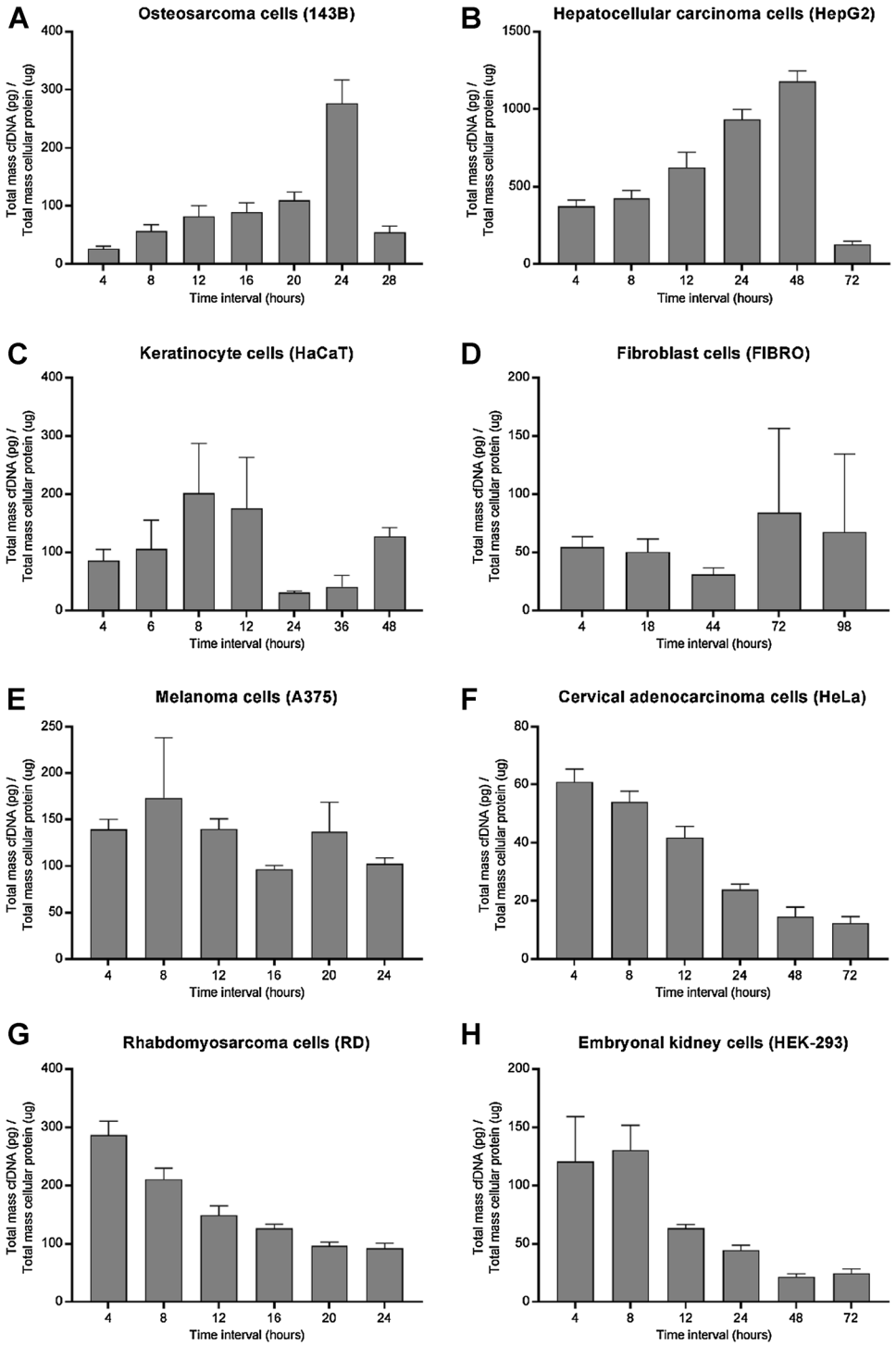

Fig. 2 CfDNA release patterns of **a** 143B quantified by qPCR using β-globin (from Bronkhorst et al. [14]), **b** HepG2, **c** HaCaT, **d** FIBRO, **e** A375, **f** HeLa, **g** RD, and **h** HEK-293 cell lines (quantified using the Qubit high sensitivity assay) after the indicated hours of incubation following medium renewal. The value of each bar represents the average (±SD, $n = 6$) amount of cfDNA released in 12 mL of growth medium normalized in terms of the total cellular protein present in the culture flask at each time interval

with both low levels of cirDNA and high levels of DNase activity and that several cancers present with increased cirDNA levels and decreased DNase activity [29–31]. Significantly increased cirDNA levels in healthy trained subjects can also be reduced by increased endogenously expressed DNase activity [31]. It is, therefore, likely that a reduction in cfDNA levels present in the growth medium of these two and the other cell lines are also likely due, in part, to increased extracellular DNase activity.

HeLa, RD, and HEK-293 cells shared similar patterns of cfDNA release, where cfDNA levels decreased initially, followed by a significant peak and a subsequent decrease as the confluence increased (Fig. 2). HeLa cells released 60 pg/µg protein (Fig. 2f) and showed an initial

decrease in cfDNA levels (ng per flask), followed by a gradual increase (Fig. 1e). RD cells produced the second highest level of cfDNA at 286 pg/μg within 4 h of incubation, similar to the level of cfDNA release from 143B cells [14] (Fig. 2g), followed by a gradual decrease in cfDNA levels (ng per flask) as time progresses (Fig. 1f). HEK-293 released 130 pg/μg protein (Fig. 2h) with an initial increase in cfDNA levels (ng per flask) during the first two time intervals (4 and 8 h), followed by a slight decrease at 12 h, a slight increase at 24 and 48 h, and a more significant increase at 48 h (Fig. 1g).

The first two cfDNA release patterns (increased and decreased cfDNA release) did not appear to have correlations with tissue origins. The cfDNA release patterns was, on the other hand, less clearly increasing or decreasing for the cell lines, HaCaT, FIBRO, and A375 cells (Fig. 2), originating from skin cells. Since both the variable cfDNA release patterns and replicate inconsistencies occurred only in HaCaT, A375, and fibroblast cells, which all originate from skin cells, the results suggest that these characteristics can be related to the skin origin of the cells. Only the skin cell lines showed more prominent signs of replicate inconsistencies likely due to unstable growth rates resulting in significant differences in the amount of cfDNA and protein extracted in the duplicate flasks. HaCat released 170–200 pg/μg protein (Fig. 2c) with an initial increase in cfDNA levels (ng per flask) at 8 h, a gradual decrease at 12, 24, and 36 h, and a significant increase at 48 h (Fig. 1b). There are, however, significant replicate inconsistencies at 4–8 h. A375 also released between 170 and 200 pg/μg protein with less significant changes in cfDNA release patterns between time intervals (Fig. 2e), fluctuating cfDNA levels (ng per flask) (Fig. 1d) and significant inconsistencies between replicate flasks at 8 h. Visually, it appears that the following pattern of cfDNA release occurs: higher levels of cfDNA were initially detected, followed by a decrease in cfDNA release and a subsequent increase as the degree of confluence of the cell lines increased (Fig. 2e). A similar experiment screening for the 24 h cfDNA release patterns of A375 quantified via qPCR using β-globin revealed the same pattern of variable cfDNA release over time during the exponential growth phase (data not shown) with similar levels of replicate inconsistencies. FIBRO cells, on the other hand, released a constant cfDNA level of around 50 pg/μg protein during the first 24 h of incubation (Fig. 2d), showing a little variation in cfDNA release patterns (pg/ μg protein) between time intervals (data not shown) that only began to slightly change after 24 h, but resulted in significant standard deviations from 72 h. The cells showed a gradual decrease in cfDNA levels (ng per flask) at 4, 18, and 44 h, followed by a significant increase at 72 h with a significant standard deviation (Fig. 1c).

Cell-free DNA fragment size evaluation

To elucidate the fragment size distribution of cfDNA, four of the cell lines, HepG2, RD, HEK-293, and FIBRO, were selected and the cfDNA isolated at the different time intervals were used to perform microchip-based capillary electrophoresis. The results were then compared to that of 143B cells from Bronkhorst et al. [14].

The electropherograms of 143B (Fig. 3), HepG2 (Fig. 4), FIBRO (Fig. 5) and, to a lesser extent, RD (Fig. 6), and HEK-293 (Fig. 7) cells showed indications of the presence of small DNA fragments (<100 bp, particularly at 47–50 bp) at each time interval. CirDNA from tumor cells have been shown to consist of DNA fragments smaller than that of healthy subjects, particularly <100 bp, and these DNA fragments largely consist of the mutated DNA originating from the tumor [32, 33]. However, the normal, noncancerous cell lines, FIBRO and HEK-293, also present with small cfDNA fragments, an observation also observed in a recent study by Underhill et al. [34], where short DNA fragments of both rat and human were detected in controls. As such, the presence of smaller DNA fragments in noncancerous cfDNA makes it difficult to discern whether or not the small fragments of the cancerous cell lines are indeed mutated tumor DNA fragments, in the absence of DNA sequencing.

HepG2 cfDNA (Fig. 4) showed a typical ladder pattern characteristic of nucleosomal subunits of predictable sizes that are most prominent at around 150–200, 300–400, and 500–600 bp. Our previous study using 143B cells revealed that apoptosis occurs in samples where this typical ladder pattern is detected [14], indicating that apoptosis could be present in the HepG2 cell cfDNA at each time interval. These peaks decreased notably from 4 to 24 h, but increased again after 48 h of incubation. Concurrently, a peak at approximately 2000 bp formed at each time interval, which increases in intensity [fluorescent units (FU)] from 4 to 24 h as the ladder pattern fragment peaks decrease, followed by an increase in FU at 48 h when the ladder pattern fragment peaks start to increase. Interestingly, both the 2000 bp peak and apoptotic peaks of the HepG2 cells decrease in FU significantly at 72 h. The 143B electropherogram data [14] correlated well with that of HepG2 cells, showing a pattern of an apoptotic DNA fragment of 166 bp that decreases as a 2000 bp peak develops. At 24 h, the 2000 bp peak is at its largest and starts to decrease at further time intervals with a concomitant increase in the apoptotic DNA fragment peaks (Fig. 3). The 2000 bp peak was found to occur in the absence of apoptosis and necrosis, possibly indicating that this peak is the actively released form of cfDNA [14].

The FIBRO samples (Fig. 5) presented with apoptotic DNA fragments and a 2000 bp disturbance from 4 h.

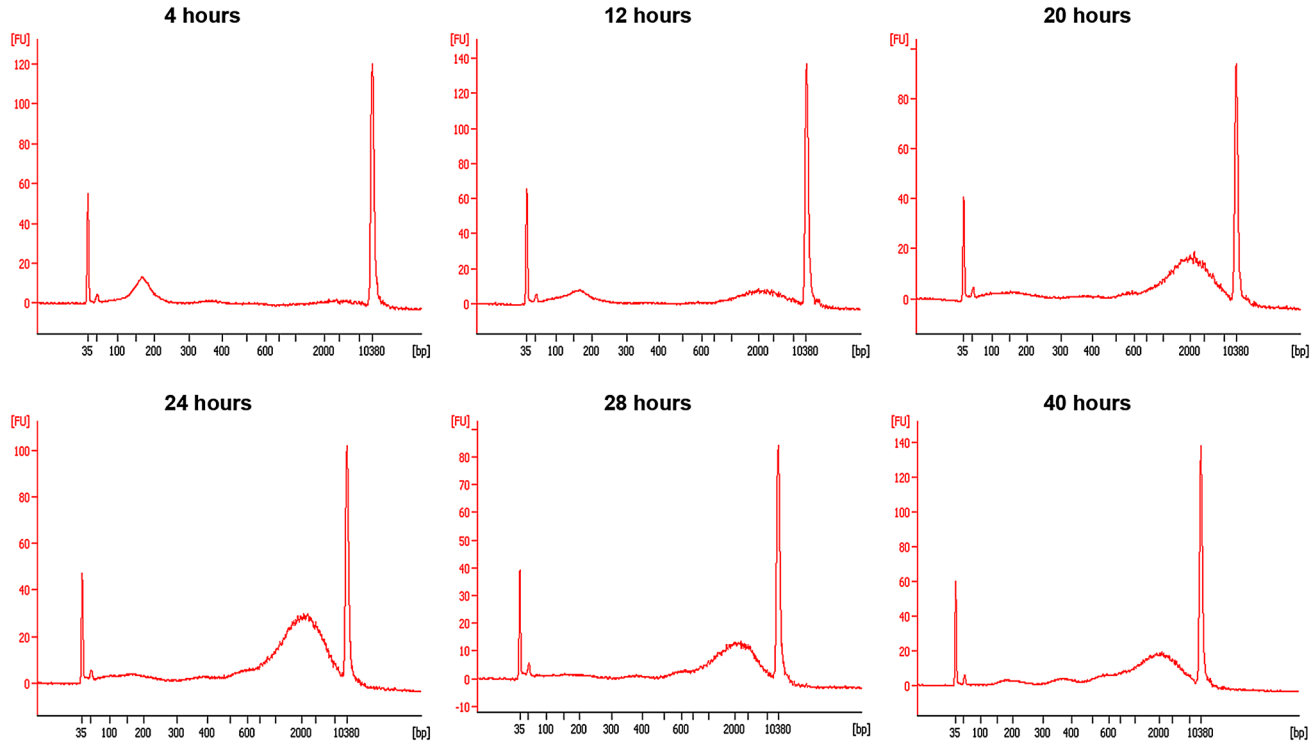

Fig. 3 Capillary electropherograms showing the fragment sizes of cfDNA isolated from 143B cells after 4–40 h of incubation following medium renewal [14]. The peak at 150–200 bp was shown to be representative of apoptosis, while larger peaks arising after 12 h of incubation and reaching a maximum at 24 h are not derived from either apoptotic or necrotic cfDNA release

Changes in the 2000 bp area are barely visible, but the nucleosomal ladder pattern peaks decrease in FU as time progresses and significantly increases at 72 h. RD cfDNA (Fig. 6) also showed a typical ladder pattern associable with nucleosomal subunits at each time interval. These peaks decreased to significantly low levels, becoming barely visible as time progressed. Concurrently, a peak at approximately 2000 bp is also present at each time interval, which increases in FU from 4 to 12 h as the apoptotic peaks decrease at 16–24 h. HEK-293 samples (Fig. 7) showed no indications of smaller DNA fragments. A peak forms at approximately 2000 bp at 4 h, which seems to gradually decrease in FU. At 72 h, however, there seems to be a more visible disturbance in the baseline from approximately 150 bp, which could indicate the initial formation of apoptotic DNA fragment peaks.

The patterns of the 2000 bp peaks, in particular, of the cell lines correlate well with the cfDNA release patterns demonstrated in Figs. 1 and 2. The 2000 bp peak of HepG2 and 143b (Figs. 3, 4) increases, followed by its decrease and concomitant increase in the other fragment peaks (less clearly visible for 143B in Fig. 2a), together forming a maximum level of cfDNA release. A later decline in all fragment peaks results in the significant drop in cfDNA levels in Fig. 2a, b. The 2000 bp peaks of RD and HEK-293 (Figs. 6, 7) and nucleosomal ladder fragment peaks of FIBRO (Fig. 5), on the other hand, decreased as time progressed, with an increase at 72 h for FIBROs, correlating with the cfDNA release patterns of Fig. 2d, f, and g. The different cfDNA release patterns are, in conclusion, not due to different ratios of apoptotic to actively released cfDNA, but primarily due to fluxes in actively released cfDNA. Electropherogram data did, therefore, not provide an explanation as to why there are different cfDNA release patterns.

Similar results have been observed in epidermoid carcinoma (A431), HeLa, human umbilical vein endothelial cells (HUVEC), human T lymphocytes (Jurkat cells), and pleural effusion cells (U937) [14, 35–37]. Morozkin et al. showed that cfDNA concentrations increase over time during the lag and beginning of the exponential growth phase of cell lines. They have also determined via electrophoretic analysis that the molecular weight of the obtained cfDNA was between 400 and 10,000 bp, suggesting that cfDNA is neither from apoptotic nor necrotic origin and is likely actively released from cells [36, 37]. Choi and colleagues, who studied their cell lines (Jurkat and U937) under normal, apoptotic, and necrotic conditions, have showed similar increases in cfDNA levels over time and that apoptosis results in a rather dramatic increases of cfDNA levels after 24–48 h of incubation in comparison with normal

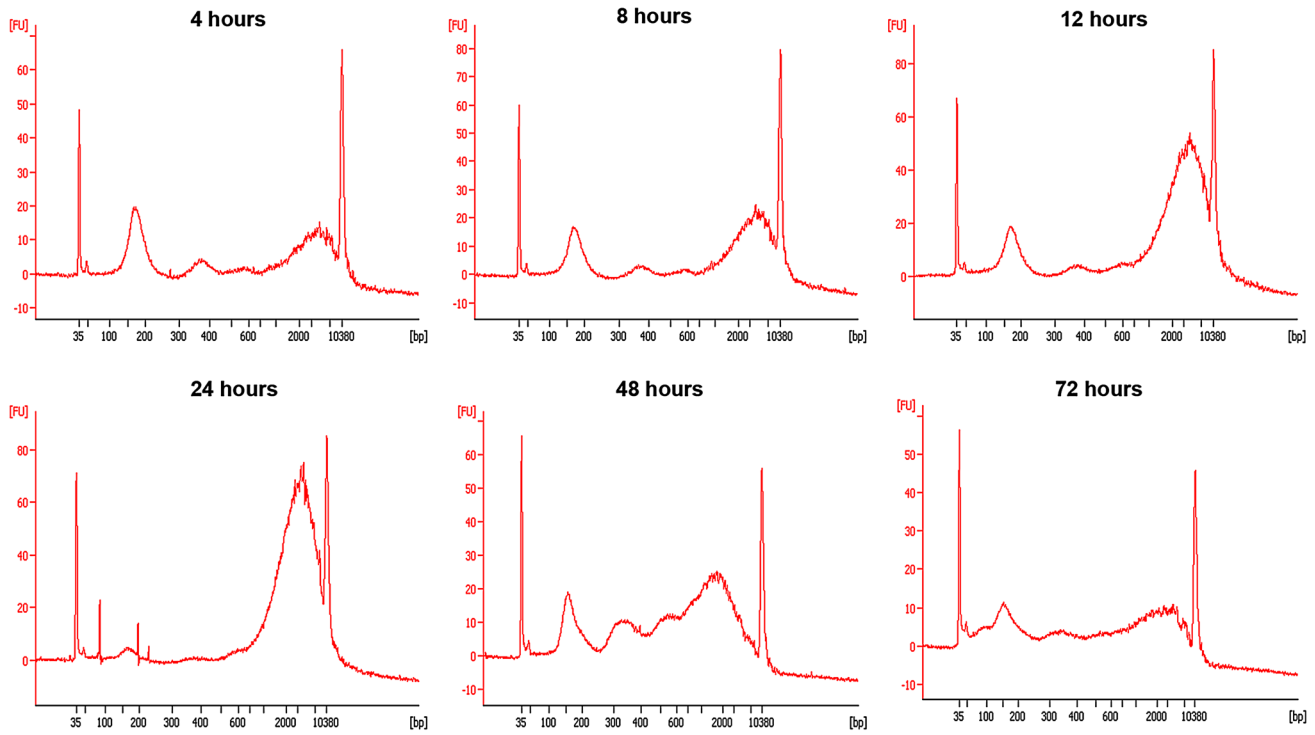

Fig. 4 Capillary electropherograms showing the fragment sizes of cfDNA isolated from HepG2 cells after 4–72 h of incubation following medium renewal. Each shows a typical ladder pattern associable with nucleosomal subunits of predictable sizes that are most prominent at around 150–200, 300–400, and 500–600 bp. After 12 h, a major peak is visible at around 2000 bp. This peak reaches a maximum of a little under 80 FU at 24 h, but then decreases, while the smaller peaks rise

or healthy cells. Necrosis, on the other hand, resulted in a decline of cfDNA levels over time, which indicated that cfDNA may be released by more than one mechanism, but that apoptosis can be primarily held responsible for high cfDNA levels [35].

The implications of apoptotic and actively released DNA fractions in circulating DNA

Little attention has been given to the impact that the different fragment sizes of cirDNA contents may have on studies in which recipient cells or animals are treated with cirDNA. For example, Mittra et al. [15] provided disconcerting evidence regarding the damaging effects cirDNA on recipient cells. Fragmented DNA and chromatin isolated from the blood of cancer patients and healthy volunteers were co-cultured with mouse fibroblasts, ovary, kidney and adipocyte cells, and HeLa cells, and were injected into mice, resulting in the induction of apoptosis. The fragmented DNA and chromatin of the healthy volunteers, however, resulted in a lower effect than that of the cancer patients. It is most likely that the DNA isolated from these subjects is of multiple intercellular origins, similar to that observed in cell lines. Studies have proposed that apoptosis serves as the source of cirDNA in both normal and diseased tissues [38]. Cells and whole organs in culture also spontaneously release nucleoprotein complexes in a homeostatic environment and newly synthesized DNA is preferentially released, indicating the presence of an active DNA release mechanism [39–42]. That being the case, the question becomes whether the apoptotic and actively released fractions of the DNA isolated will both result in damaging effects in vitro and/or in vivo or whether the damaging effects observed by Mittra et al. [15] were due to only one of the fractions.

Are both apoptotic and actively released DNA fractions responsible for damaging effects?

Although both healthy and tumor cells can undergo apoptosis, the levels of apoptosis in cancer patients will likely be higher than in healthy patients due to increased stress levels and/or decreased vascularization in both the tumors and surrounding tissues [43]. This could explain why the DNA isolated from the healthy volunteers had a less prominent effect on recipient cells and mice than that of the cancer patients. Bystander effect (the effect of information transfer from targeted cells exposed to damaging agents of physical nature or chemical nature to surrounding, non-irradiated cells) studies have shown similar damaging consequences when DNA released from irradiated cells are given to

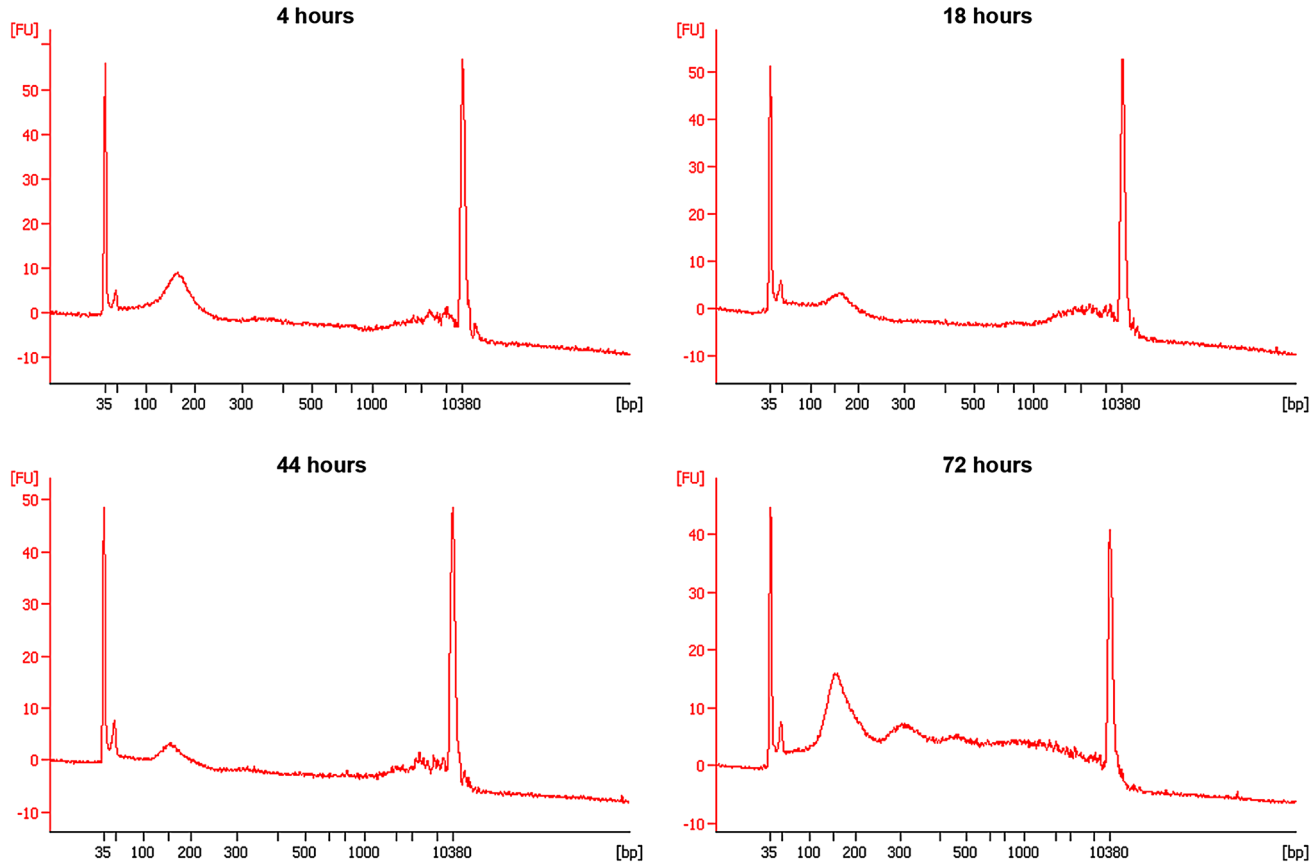

Fig. 5 Capillary electropherograms showing the sizes of cfDNA isolated from FIBRO cells after 4–72 h of incubation following medium renewal. Very prominent in each electropherogram is the peak at 100–200 bp. This peak is associable with apoptosis and becomes exceptionally prominent at 72 h of incubation. Also visible in each electropherogram is a typical ladder patter associable with multiple nucleosomal subunits. The entire baseline is elevated at 72 h of incubation as an indication of the presence of variable fragment sizes ranging from 35 to 10,000 bp

non-irradiated recipient cells [44–46]. Contrarily, Garcia-Olmo et al. [47] showed that newly synthesized and/or spontaneously released virtosomes from non-dividing cells reduced tumor growth and metastasis, but had little effect on normal dividing fibroblasts. This shows that actively released DNA may not have the damaging effects seen by Mittra et al. and during the bystander effect studies. It may also suggest that the effects of the different fractions of cfDNA may be dependent on the biology (type of cell) or status (healthy or diseased) of the recipient.

Puszyk et al. [48] and Bronkhorst et al. [49] showed that selectivity may be involved in the release of cfDNA, as there is an unequal representation of cfDNA sequences and genes in the blood samples of humans and culture growth medium, respectively. The transfer of cfDNA between different cells and recipients has been demonstrated both in vitro and in vivo on multiple occasions (refer to Bronkhorst et al. [14]), and the bystander effect studies and tumor growth inhibition effects of the cfDNA of non-dividing cells mentioned above further support the idea of cfDNA serving as an intercellular messenger of sorts, a concept that has been considered on occasion [11, 50] and that both actively released cfDNA and apoptosis-derived cfDNA may serve different purposes in a cellular environment. The elucidation of the separate effects of actively released and apoptosis-derived cfDNA fractions is, therefore, strongly encouraged to better understand the true biological role and clinical implications of cfDNA. For this reason, the utilization of cell cultures instead of (or in conjunction with) plasma or serum samples is strongly encouraged.

The utilization of in vitro cell cultures in circulating DNA research

Standard two-dimensional (2D) cell cultures have significant benefits for cirDNA research. It has been demonstrated that the contents of cell culture cfDNA and plasma sample cirDNA are very similar, as the electropherograms of plasma samples show the same patterns of nucleosomal ladder fragments and a prominent 2000 bp peak detected

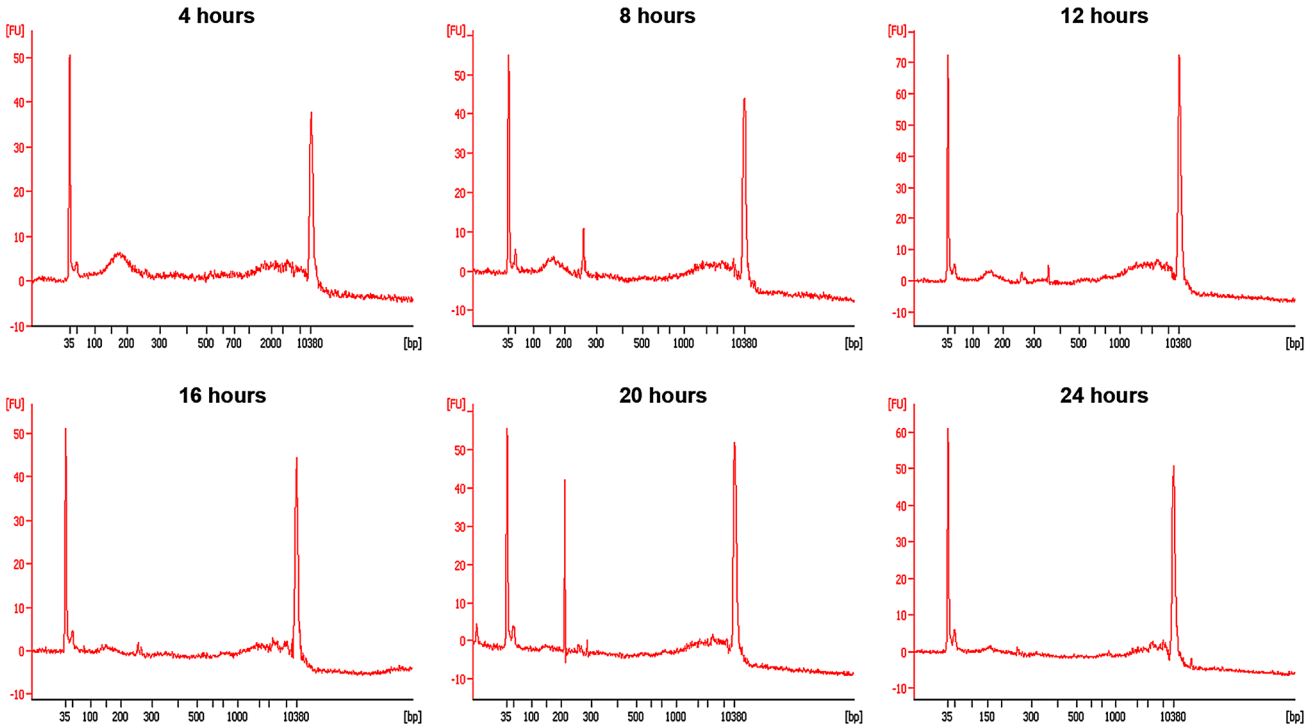

Fig. 6 Capillary electropherograms showing the fragment sizes of cfDNA isolated from RD cells after 4–24 h of incubation following medium renewal. A peak is prominent at 100–200 bp from 4 h of incubation that has been shown to be associable with apoptosis [14]. This peak can be seen declining over time, reaching a barely visible amplitude at 24 h of incubation. In these electropherograms, the baseline appears 'disturbed' throughout all time intervals. Also visible from the 4 h interval is a peak with a maximum amplitude at the 2000 bp range that has previously been shown to be unassociated with apoptotically and necrotically derived cfDNA. While the 2000 bp peak declines, peaks at lower increments of nucleosomal subunits again appear more prominent

in this study's eight cell lines [51]. These similarities in cfDNA and cirDNA contents are, however, dependent on the extraction methods used as the choice of extraction method may cause bias in blood-based studies. The Kingfisher method, for example, failed to extract cfDNA with a size of 2000 bp [51]. Furthermore, the origins of the cfDNA in the growth medium of 2D cultures are restricted to a particular tissue origin, cell morphology, and disease, thereby providing "more focused" sample contents that may simplify or aid the discovery of biological markers, the elucidation of biological functions, and the potential determination of the effects of cell morphology on cirDNA characteristics. Recent experiments screening the cfDNA characteristics of three-dimensional (3D) cell cultures have shown that the cfDNA of spheroids, developed with HepG2/C3A cells in microgravity bioreactors [52], effectively mirrors the brief and/or minor changes in the growth and glucose consumption during spheroid development and toxicological studies (unpublished data). Moreover, the fragment patterns of the spheroid cfDNA correlate with that of both 2D cell cultures and human plasma samples. An extension from 2D cell cultures to 3D in vitro models prior to in vivo research can, therefore, also be of great value to the cirDNA research field as one will be able to obtain more physiologically relevant samples while still having the benefit of a restricted environment of a specific cellular origin or disease.

Bioenergetic analyses

Mito stress test

Six parameters were calculated using the Mito stress test OCR results, namely: basal respiration (last OCR measurement prior to oligomycin injection), proton leak (the minimum OCR measurement following oligomycin injection), ATP production (proton leak subtracted from basal respiration), maximal respiration (the maximum OCR measurement following FCCP injection), and spare respiratory capacity (maximal respiration minus basal respiration). The sixth parameter, non-mitochondrial respiration (the minimum OCR measurement following rotenone/antimycin A injection), was an indication of all oxygen being consumed by processes independent of the OXPHOS system and was thus subtracted from the other five Mito stress test parameters. The OCR results for each of the OXPHOS parameters

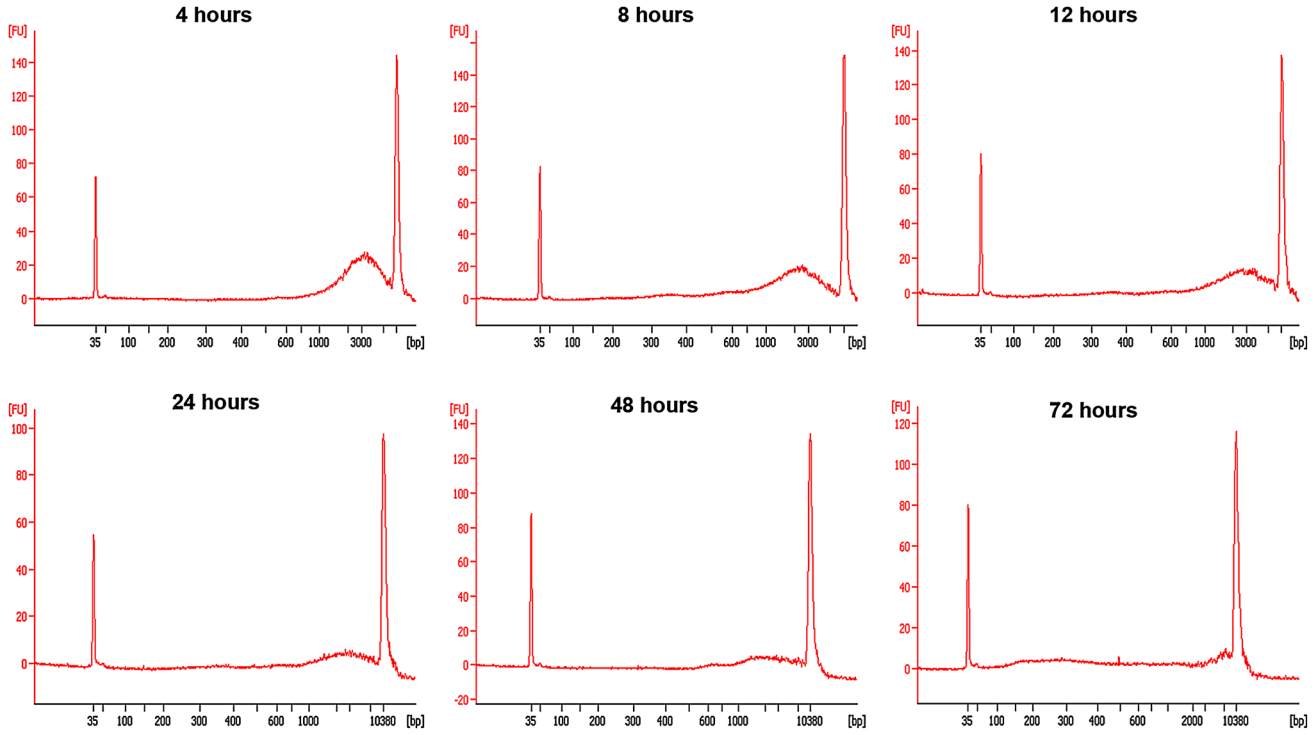

Fig. 7 Capillary electropherograms showing the sizes of cfDNA isolated from HEK-293 cells after 4–72 h of incubation following medium renewal. The electropherograms show no indications of smaller peaks. Instead, a peak with maximal fluorescence is visible at 2000–3000 bp. Once again, this peak diminishes over time, while slight disturbances in the baseline become visible after 8 h of incubation

for each cell line are illustrated in Fig. 8. HepG2, FIBRO, 143B, and RD cells were shown to have low OXPHOS activity, indicating that these cancer cells and fibroblasts may have a greater dependence for glycolysis as an energy source. HeLa and A375 showed slightly higher levels of OXPHOS activity, which may indicate that these cancer cell lines have a more moderate need for both OXPHOS and glycolysis for energy production. HaCaT and HEK-293 presented high OXPHOS activity, which is expected for normal or healthy cells. These results are discussed in "Correlation between bioenergetics results and cell-free DNA release".

Glycolysis stress test

Five parameters were calculated using the glycolysis stress test ECAR results, namely: glycolysis (maximum ECAR measurement following glucose injection), glycolytic capacity (maximum ECAR measurement following oligomycin injection), glycolytic reserve (glycolytic capacity minus glycolysis), and glycolytic reserve as a %. The non-glycolytic acidification (last measurement prior to glucose injection) was subtracted from all other glycolytic parameters. The ECAR results for each of the glycolytic parameters for each cell line are illustrated in Fig. 9.

HepG2, A375, and HEK-293 cells showed high levels of glycolysis and glycolytic capacity. The high glycolysis and significantly low OXPHOS activity of HepG2 cells, with a significantly slow growth rate, correlate well with the theory of cancer cell lines utilizing aerobic glycolysis as a predominant energy source. The moderate glycolysis and OXPHOS levels of RD are also indicative of this cancer cell line's slow growth rate and larger dependence on glycolysis. The high levels of glycolysis activity and moderate levels of OXPHOS activity in A375 show that higher levels of glycolysis are, indeed, required for these fast growing cancer cells, but that the glycolysis is not exclusive and that these cells can also use OXPHOS to a better extent than HepG2 cells. HeLa cells also showed moderate OXPHOS and glycolysis activity, supporting the proposal that this cell line does not necessarily have a predominant form of energy production as expected for cancer cells. 143B cells, with a growth rate similar to that of A375 cells, presented with slightly lower OXPHOS and considerably lower glycolysis levels compared to A375 cells. HaCaT cells showed moderately high levels of both OXPHOS and glycolysis activity, which is expected for normal cell lines. HEK-293 cells, however, shows significantly higher levels of both glycolysis and OXPHOS activity, which may indicate higher levels of anabolism in these cell lines compared to

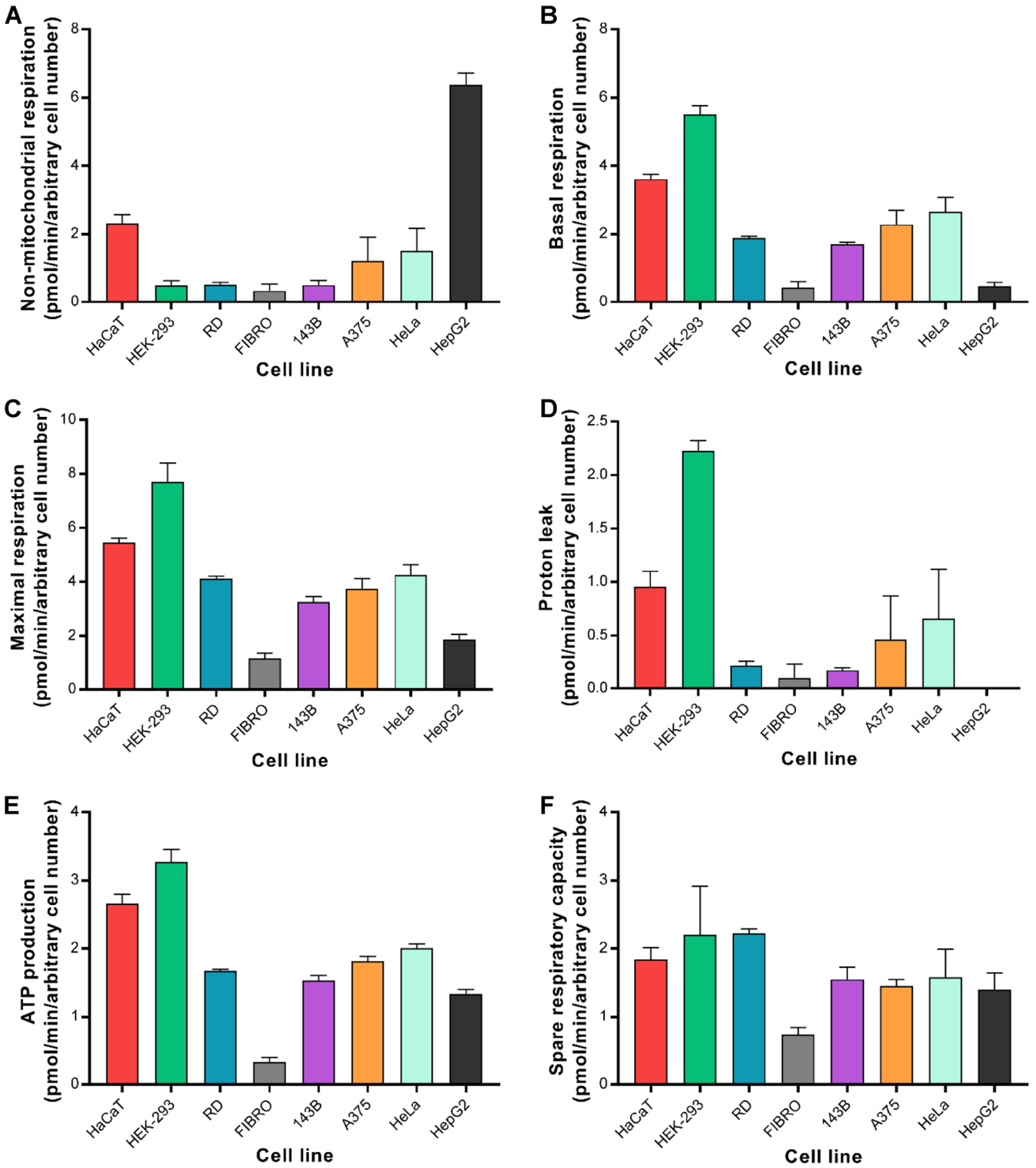

Fig. 8 Histograms depicting eight cell lines for each of the OXPHOS parameters determined using the Mito stress test ($n = 5$–6). **a** Non-mitochondrial respiration, **b** basal respiration, **c** maximal respiration, **d** proton leak, **e** ATP production, and **f** spare respiratory capacity. *Error bars* indicate standard deviation

HaCaT cells. FIBRO cells presented with the lowest level of glycolysis than that of the other seven cell lines, most likely due to its slow growth rate. Combined with its low OXPHOS levels, the bioenergetics analysis indicates that this normal skin fibroblast cell line shares metabolic similarities to cancer cells, with a higher need for glycolysis.

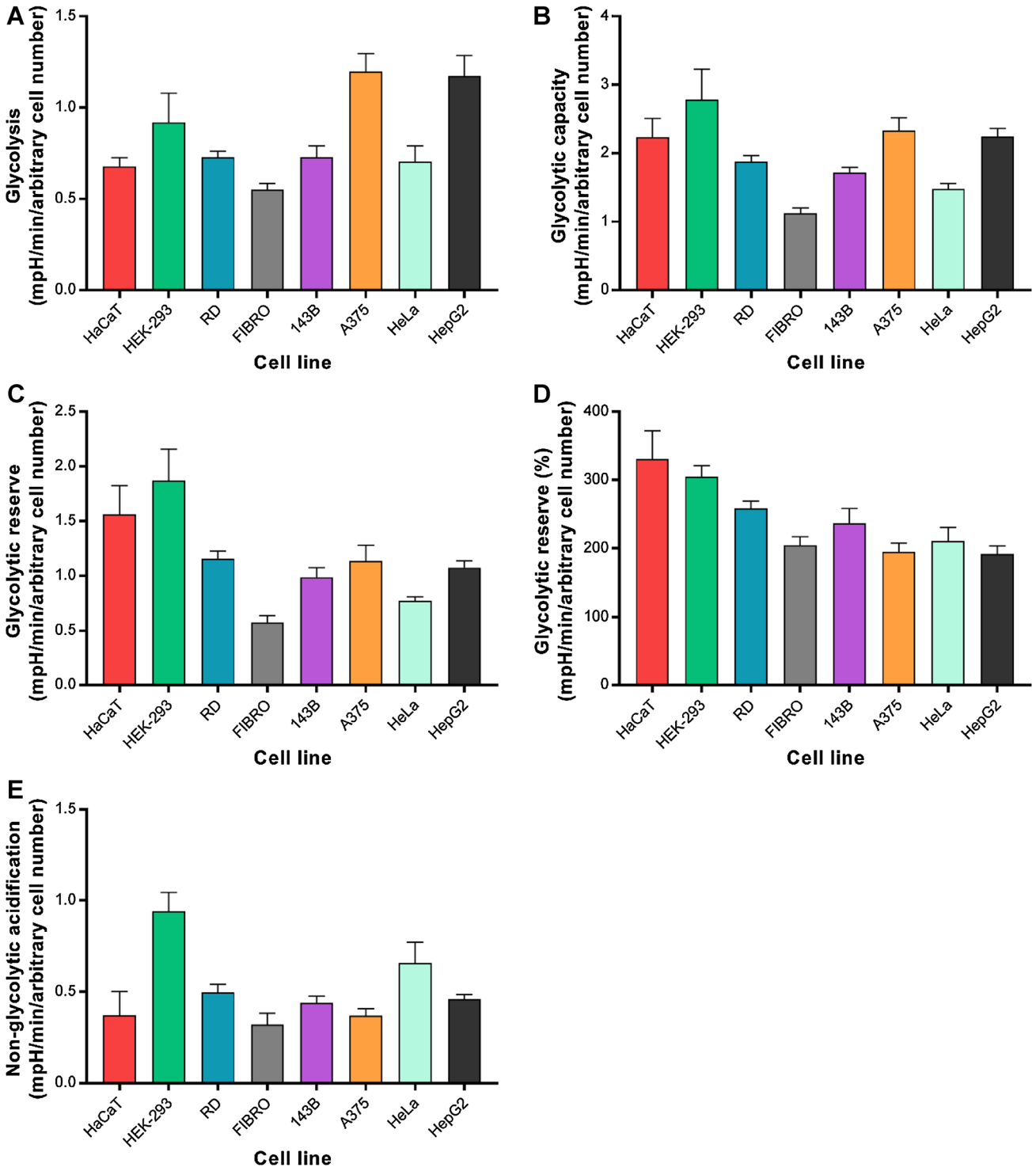

Fig. 9 Histograms depicting eight cell lines for each of the glycolytic parameters determined using the glycolysis stress test ($n = 5$–6). **a** Glycolysis, **b** glycolytic capacity, **c** glycolytic reserve, **d** glycolytic reserve (%), and **e** non-glycolytic acidification. *Error bars* indicate standard deviation

These results were used and further explained in the following section.

Correlation between bioenergetics results and cell-free DNA release

The bioenergetics results obtained in "Mito stress test" and "Glycolysis stress test" were correlated to the respective amounts of cfDNA released at 24 h of incubation (see "Cell-free DNA release patterns"), since the XF analysis was conducted 24 h after cell seeding, using Pearson's correlation coefficient, as shown in Table 1. The only parameter revealing a significant correlation was non-mitochondrial respiration, an indicator of other cellular processes outside of the mitochondrion which consume oxygen, and a scatter plot of this is given in Fig. 10. Scatter plots were constructed for each bioenergetic parameter against cfDNA yield (data not shown) and it was observed that while glycolysis did not show a significant correlation when using all eight cell lines, there did appear to be a trend when splitting the eight cell lines into two groups, namely group 1 (HEPG2, 143B, RD, and FIBRO) and group 2 (HEK-293, A375, HaCaT, and HeLa).

Since no significant correlations were seen between any of the OXPHOS parameters and cfDNA release, besides non-mitochondrial respiration, there does not appear to be a link between cfDNA release and the electron transport chain's capacity for substrate oxidation and meeting the energy demands of the cell. Non-mitochondrial oxygen consumption is believed to be due to certain detoxification, pro-inflammatory, and desaturase enzymes that consume oxygen outside of the OXPHOS system and tend to increase when subjected to stressors such as ROS [53]. It is generally a parameter that provides relatively low OCR values. As can be seen by Fig. 8a, the non-mitochondrial OCR values for the HEK-293, RD, FIBRO, and 143B cell lines are very low and similar, while the HaCaT, A375, and HeLa cells lie slightly higher. In Fig. 10, the HEPG2 cells can be seen to have much greater cfDNA levels and non-mitochondrial respiration compared to all the other cell lines. When removing the HEPG2 cell line from the correlation analysis, the significant correlation that was originally observed (Table 1) is then lost ($p = 0.379$). When studying Fig. 10b, one can also see that when looking at group 2 only (which excludes the HepG2 cell line), there does not appear to be a linear correlation and the HepG2

Table 1 Pearson's correlation coefficient and *p* values for eight cell lines testing the correlation between each bioenergetic parameter and the cfDNA release at 24 h[a]

OXPHOS parameters			Glycolytic parameters		
Statistic	*r*	*p* value	Statistic	*r*	*p* value
Non-mitochondrial respiration	0.8739	0.05	Glycolysis	0.5729	0.14
Basal respiration	−0.5124	0.19	Glycolytic capacity	0.1731	0.68
Maximal respiration	−0.4663	0.24	Glycolytic reserve	−0.1084	0.80
Proton leak	−0.6870	0.06	Glycolytic reserve (%)	−0.4237	0.30
ATP production	−0.2836	0.50	Non-glycolytic acidification	−0.1533	0.72
Spare respiratory capacity	−0.1987	0.64			

[a]The cfDNA data at 18 h was used for FIBRO, since data at 24 h was not available

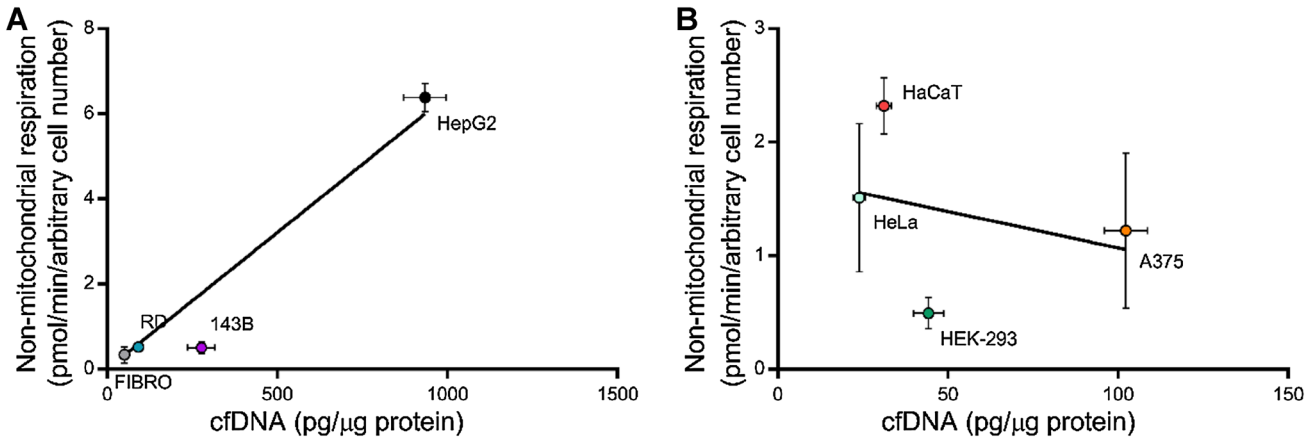

Fig. 10 Scatter plot depicting the correlation between non-mitochondrial respiration and cfDNA release for **a** group 1 (HEPG2, FIBRO, RD, and 143B) and **b** group 2 (HeLa, HaCaT, A375, and HEK-293). Values indicate the mean ± standard deviation

cell line was thus most likely skewing the data. Due to the markedly increased non-mitochondrial respiration and cfDNA levels of the HepG2 cells, there does appear to be a correlation, but this does not appear to be true for the other cell lines. Increased non-mitochondrial respiration is believed to negatively affect the bioenergetic status of cells, which is demonstrated in Fig. 8b, c, and e, where the basal respiration, maximal respiration, and ATP production were lower in the HepG2 cells compared to all the other cell lines (with the exception of FIBROs).

As shown in Table 1, a positive correlation could be seen for glycolysis and cfDNA release, but this correlation was, however, not statistically significant. As shown in Fig. 11a and b, when these two groups are separated, there is a statistically significant positive correlation with a very high effect size for both group 1 ($r=0.9703$, $p=0.030$) and group 2 ($r=0.9643$, $p=0.036$). When studying all of the other bioenergetics parameters relative to these two groups, no other statistically significant differences were observed. It would thus appear that greater cfDNA release occurred in cell lines with increased glycolytic rates. Glycolysis was determined by injecting a saturating concentration of glucose into the media (which did not initially contain glucose or pyruvate) and measuring the rate by which lactate production increased following the glucose injection (which was then converted to pyruvate and then to lactate).

It is interesting to note that the grouping of the cell lines into group 1 and 2 correlates not only with the bioenergetics analysis data obtained in "Mito stress test" and "Glycolysis stress test", but also with the cfDNA release patterns of "Cell-free DNA release patterns" and "Cell-free DNA fragment size evaluation". Group 1's HepG2, 143B, RD, and FIBRO cells presented with low OXPHOS activity and more predominant glycolysis dependence as energy source. Group 2's HEK-293, A375, HaCaT, and HeLa showed less dependence towards any specific energy source, with moderate-to-high levels of both OXPHOS and glycolysis. In addition, group 1 consists of the three cell lines (with the exception of RD) that presented with increasing levels of cfDNA release and group 2 consists of the cell lines (with the exception of HaCaT) that presented with decreasing levels of cfDNA release as the cells increases in confluence. The increasing or decreasing patterns of cfDNA release and active cfDNA release levels of cell lines, therefore, correlate with glycolysis activity. What is even more interesting to note is that the screening of potential housekeeping genes as reference genes for PCR-based quantification of cfDNA revealed that cell lines did not release SDHA, ATP5B, and CYC1 (housekeeping genes related to OXPHOS) into culture media, but were expressed by the cultured cells [49], which may explain or contribute to the lack of correlations found between cfDNA release and OXPHOS activity.

One of the limitations of this study was that bioenergetic analyses could only be performed after 24 h due to the specifications of the instrument. This correlation between glycolysis and cfDNA could be better confirmed if the bioenergetics of each cell line could be determined at the same time intervals as those used for cfDNA release and a consistent correlation can be seen.

Potential mechanisms for cell-free DNA release—glycolysis correlations

Aerobic glycolysis versus regular cellular metabolism To date, it is well known that aerobic glycolysis in cancer cells results in the increased consumption of glucose and glutamine, with very little glucose being used for OXPHOS [22–24]. This correlates well to the correlation found between glycolysis and cfDNA release of the cell lines in group 1 (Fig. 11) cell lines HepG2, 143B, and RD and, interestingly, normal fibroblasts. Proliferating fibroblasts rely on

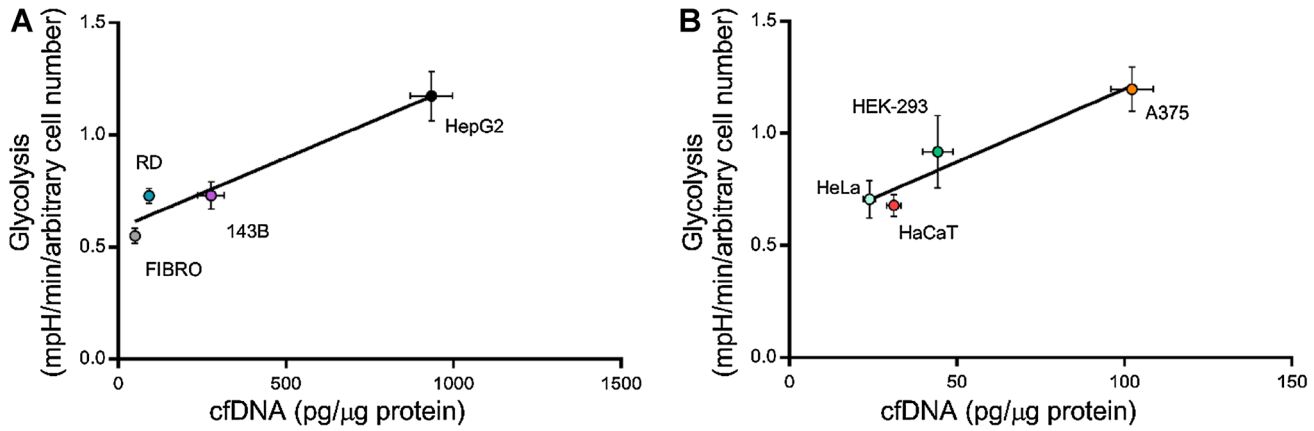

Fig. 11 Scatter plots depicting the correlation between glycolysis and cfDNA release for **a** group 1 (HEPG2, FIBRO, RD, and 143B) and **b** group 2 (HeLa, HaCaT, A375, and HEK-293). Values indicate the mean ± standard deviation

the pentose phosphate pathway to generate ribose for nucleotide synthesis [54]. The glucose and glutamine metabolism in the TCA cycle of proliferating fibroblasts is interrupted at the citrate step and glutamine is primarily used for anaplerosis (process that ensures the replenishment of TCA cycle intermediates) [55]. Fibroblasts also require higher glucose levels due to their high energy consuming function of producing large amounts of extracellular matrix components [54]. These factors may explain why FIBRO cfDNA levels correlated to glycolysis levels along with that of the cancer cell lines, whereas the normal cell lines, HaCaT and HEK-293, showed correlations in group 2 (Fig. 11) due to normal energy metabolism functions.

The cancer cell lines HeLa and A375, on the other hand, formed part of the correlation in group 2. HeLa and HaCaT cells have been shown to have similar central carbon metabolism enzyme activities, but HeLa cells showed an upregulation in almost all of the central carbon metabolism's enzymes using fructose 6-phosphate as a substrate [56]. It should, therefore, be more beneficial for HeLa cells to limit ATP production via the TCA cycle to maintain a more active phosphofructokinase. However, increased ATP utilization linked to cell proliferation results in increased ATP production rates via the pentose phosphate pathway. The similarities between enzyme activity of HaCaT and HeLa cells may indicate that the aerobic glycolysis dependence of HeLa cells may be less prominent than that of the other cancer cell lines, explaining or contributing to the lack of correlation between cfDNA release and glycolysis levels in HeLa cells. A375 cells may also serve as an example of cancer cells that do not primarily depend on aerobic glycolysis, as they presented with moderate levels of OXPHOS activity and their high glycolysis levels are likely due to their fast growth rate.

The involvement of other factors correlating to glycolytic activity Due to the complex nature of the cell and the numerous intra-, inter-, and extracellular factors that play a role, it is understandable that a correlation was only seen in one of the many bioenergetic parameters that were tested, and that other factors than cfDNA release that can correlate with glycolytic activity may have contributed to the observed glycolysis-cfDNA release correlation, e.g., apoptosis and proliferation capacity.

The electropherogram data of "Cell-free DNA fragment size evaluation" indicate that the ratio of apoptotic cfDNA fragments to the 2000 bp fragments (actively released cfDNA) is significantly low for the tested cell lines at 24 h. Apoptosis is, therefore, unlikely to serve as a contributing factor towards the observed correlations. While the underlying reason for this correlation is unclear, it would appear that the proliferating capacity of the cell lines may play a role. De Preter et al. [20] found that increased proliferation capacity (as measured by DNA synthesis) was significantly correlated to increased glycolysis but did not have a significant correlation to mitochondrial respiration. No analyses were performed to assess the proliferative capacity of each cell line, but this may be a useful approach to investigate in the future in conjunction with cfDNA release and glycolysis.

In vivo considerations that may affect the glycolysis—cell-free DNA release correlation

Whether cfDNA release will correlate with glycolytic activity in an in vivo setting requires investigation. There are several in vivo factors that can either mask or negate the observed correlations. First, whereas 2D cell cultures consists of specific cell morphologies or types, organ tissues and tumors consist of various cell types and morphologies, each likely to have its own level of contribution to the cfDNA sample and its own preference to glycolysis or OXPHOS activity. Second, the monolayer of cells in cultures cancels out the effects of both effective and ineffective circulation, respiration and clearance of nutrients, oxygen, and metabolites on cellular activity in healthy tissues and tumors, which will likely affect cirDNA release patterns. Finally, the utilization of adjacent, healthy cells as metabolic intermediate donors and self-digestion [13] to fuel tumor cells can also affect or alter the relationship between cellular metabolism and, in effect, cirDNA release. As discussed in "The utilization of in vitro cell cultures in circulating DNA research", there are 3D culture methods that can be used to effectively simulate these conditions whilst having a source of released DNA restricted to that of the targeted tissue or disease. The initial use of 3D cultures to study the relationship between cellular metabolism and cfDNA or cirDNA release before diverting to plasma samples may provide a necessary step-by-step progression in terms sample complexity required to finally elucidate the biological function of cirDNA.

Conclusions

To summarise, three distinct cfDNA release patterns were detected, namely (1) increased, (2) decreased, and (3) variable levels of cfDNA levels over time during the exponential growth phase of cell lines of different origins. The variable cfDNA release patterns occur in HaCaT, A375, and fibroblast cells, and are, therefore, theorized to be related to the skin origin of the cells. Patterns of apoptotic DNA laddering and a 2000 bp peak have been detected in all seven cell lines. As time progressed, increases in the 2000 bp peak are concomitantly followed by a decrease in nucleosomal ladder fragment peaks and vice versa. These

patterns of DNA fragment peak formations and losses correlate with the cfDNA release patterns presented for 143B cells [14] and correlate with the following observations made by Choi et al. [35–37]: (a) the cfDNA fragments of approximately 2000 bp in length are not of apoptotic or necrotic origin, (b) are likely released into the culture media via an active release mechanism, and (c) cfDNA is, therefore, released by more than one mechanism, primarily apoptosis and active DNA release. The strong similarities between cell culture cfDNA and plasma cirDNA, and the obvious implications of more than one source of cfDNA in samples, indicate that there should not be any concerns regarding the efficient translation of in vitro results into in vivo application and that cell culture models can be efficiently used instead of (or in conjunction with) biofluid samples for cirDNA research. Furthermore, we report that there were no statistically significant correlations between cfDNA release and OXPHOS, although there appears to be a slight tendency toward an inverse correlation between cfDNA release and ATP production. There is, however, a statistically significant correlation between glycolysis and the cfDNA release levels of HepG2, RD, 143B, and FIBRO cell lines that was attributed to aerobic glycolysis utilization of the cell lines, and between glycolysis and the cfDNA release levels of HaCaT, HEK-293, HeLa, and A375 cell lines, which is attributed to the normal energy metabolism activities of normal cells and lesser dependence of the cancer cells in question towards aerobic glycolysis. It is, therefore, concluded that a cell line's increasing or decreasing pattern of cfDNA release and its active cfDNA release levels correlate with the growth rate and cancer status of the cell line through its dependence on glycolytic activity.

Acknowledgements This work was supported by the National Research Foundation (NRF), South Africa [Grant Numbers SFH14061869958, SFH13092447078]. The financial assistance of the NRF is hereby acknowledged. Opinions expressed and conclusions arrived at are those of the authors and are not to be attributed to the NRF.

Compliance with ethical standards

Conflict of interest The authors declare no conflict of interest.

References

1. Mandel P, Métais P (1948) Les acides nucléiques du plasma sanguin chez l'homme [The nucleic acids of blood plasma in humans]. Compte Rendu de l'Academie des Sciences 142:241–243
2. Aucamp J, Bronkhorst AJ, Badenhorst CPS, Pretorius PJ (2016) Historical and evolutionary perspective on the biological significance of circulating DNA and extracellular vesicles. Cell Mol Life Sci 73:4355–4381
3. Lo YMD, Chan KCA, Sun H, Chen EZ, Jiang P, Lun FMF, Zheng YW, Leung TY, Lau TK, Cantor CR, Chu RWK (2010) Maternal plasma DNA sequencing reveals the genome-wide genetic and mutational profile of the fetus. Sci Transl Med 2:61ra91. doi:10.1126/scitranslmed.3001720
4. Brown P (2016) Cobas® EGFR mutation test v2 assay. Future Oncol 12(4):451–452
5. Lowes LE, Bratman SV, Dittamore R, Done S, Kelley SO, Mai S, Morin RD, Wyatt AW, Allan AL (2016) Circulating tumor cells (CTC) and cell-free DNA (cfDNA) workshop 2016: scientific opportunities and logistics for cancer clinical trial incorporation. Int J Mol Sci 17:1505. doi:10.3390/ijms17091505
6. Bronkhorst AJ, Aucamp J, Pretorius PJ (2015) Cell-free DNA: preanalytical variables. Clin Chim Acta 450(2015):243–253
7. Bronkhorst AJ, Aucamp J, Pretorius PJ (2016) Adjustments to the preanalytical phase of quantitative cell-free DNA analysis. Data Brief 6 (2016):326–329
8. Elshimali YI, Khaddour H, Sarkissyan M, Wu Y, Vadgama JV (2013) Clinical utilization of circulating cell free DNA (CCFDNA) in blood of cancer patients. Int J Mol Sci 14:18925–18958
9. Fleischhacker M, Schmidt B (2007) Circulating nucleic acids (CNAs) and cancer—a survey. Biochim Biophys Acta 1775:181–232
10. Messaoudi SE, Thierry AR (2014) Pre-analytical requirements for analysing nucleic acids from blood. In: Gahan PB (ed) Circulating nucleic acids in early diagnosis, prognosis and treatment monitoring, vol 5. Springer, The Netherlands, pp 45–69
11. Peters DL, Pretorius PJ (2012) Continuous adaptation through genetic communication—a putative role for cell-free DNA. Expert Opin Biol Ther 12:S127–S132
12. Van der Vaart M, Pretorius PJ (2010) Is the role of circulating DNA as a biomarker of cancer being prematurely overrated? Clin Biochem 43(2010):26–36
13. Thierry AR, El Messaoudi S, Gahan PB, Anker P, Stroun M (2016) Origins, structures, and functions of circulating DNA in oncology. Cancer Metastasis Rev 35(3):347–376
14. Bronkhorst AJ, Wentzel JF, Aucamp J, Van Dyk E, Du Plessis L, Pretorius PJ (2016) Characterization of the cell-free DNA released by cultured cancer cells. Biochim Biophys Acta 1863(2016):157–165
15. Mittra I, Khare NK, Raghuram GV, Chaubal R, Khambatti F, Gupta D, Gaikwad A, Prasannan P, Singh A, Iyer A, Singh A, Upadhyay P, Nair NK, Mishra PK, Dutt A (2015) Circulating nucleic acids damage DNA of healthy cells by integrating into their genomes. J Biosci 40(1):91–111
16. Collins LV, Hajizadeh S, Holme E, Jonsson IM, Tarkowski A (2004) Endogenously oxidized mitochondrial DNA induces in vivo and in vitro inflammatory responses. J Leukoc Biol 75:995–1000
17. Malik AN, Parsade CK, Ajaz S, Crosby-Nwaobi R, Gnudi L, Czajka A, Livaprasad S (2015) Altered circulating mitochondrial DNA and increased inflammation in patients with diabetic retinopathy. Diabetes Res Clin Pract 110(3):257–265. doi:10.1016/j.diabres.2015.10.006
18. Oka T, Hikoso S, Yamaguchi O, Taneike M, Takeda T, Tamai T, Oyabu J, Murakawa T, Nakayama H, Nishida K, Akira S, Yamamoto A, Komuro I, Otsu K (2012) Mitochondrial DNA that escapes from autophagy causes inflammation and heart failure. Nature 485:251–256
19. Peters DL, Pretorius PJ (2011) Origin, translocation and destination of extracellular occurring DNA—a new paradigm in genetic behaviour. Clin Chim Acta 412:806–811
20. De Preter G, Neveu MA, Danhier P, Brisson L, Payen VL, Porporato PE, Jordan BF, Sonveaux P, Gallez B (2015) Inhibition of the pentose phosphate pathway by dichloroacetate unravels a

missing link between aerobic glycolysis and cancer cell proliferation. Oncotarget 7(3):2910–2920
21. DeBerardinis RJ, Lum JJ, Hatzivassiliou G, Thompson CB (2008) Biology of cancer: metabolic reprogramming fuels cell growth and proliferation. Cell Metab 7:11–20
22. Jin L, Alesi GN, Kang S (2015) Glutaminolysis as a target for cancer therapy. Oncogene 35(28):3619–3625
23. Michalopoulou E, Bulusu V, Kamphorst JJ (2016) Metabolic scavenging by cancer cells: when the going gets tough, the tough keep eating. Br J Cancer 115:636–640
24. Muñoz-Pinedo C, Mjiyad NE, Ricci JE (2012) Cancer metabolism: current perspectives and future directions. Cell Death Dis 3:e248. doi:10.1038/cddis.2011.123
25. Gill KS, Fernandes P, O'Donovan TR, McKenna SL, Doddakula KK, Power DG, Soden DM, Forde PF (2016) Glycolysis inhibition as a cancer treatment and its role in an anti-tumour immune response. Biochim Biophys Acta 1866(2016):87–105
26. Zhao Y, Butler EB, Tan M (2013) Targeting cellular metabolism to improve cancer therapeutics. Cell Death Dis 4:e532. doi:10.1038/cddis.2013.60
27. Zandberg L, Van Dyk HC, Van der Westhuizen FH, Van Dijk AA (2016) 3-Methylcrotonyl-CoA carboxylase-deficient human skin fibroblast transcriptome reveals underlying mitochondrial dysfunction and oxidative stress. Int J Biochem Cell Biol 78:116–129
28. Tukey JW (1977) Exploratory data analysis. Addison-Wesley, Reading
29. Tamkovich SN, Cherepanova AV, Kolesnikova EV, Rykova EY, Psyhnyi DV, Vlassov VV, Laktionov PP (2006) CirDNA and DNase activity in human blood. Ann NY Acad Sci 1075:191–196
30. Cherepanova AV, Tamkovich SN, Bryzgunova OE, Vlassov VV, Laktionov PP (2008) Deoxyribonuclease activity and circulating DNA concentration in blood plasma of patients with prostate tumors. Ann NY Acad Sci 1137:218–221
31. Velders M, Treff G, Machus K, Bosnyák E, Steinacker J, Schumann U (2014) Exercise is a potent stimulus for enhancing circulating DNase activity. Clin Biochem 47:471–474
32. Mouliere F, Robert B, Peyrotte EA, Rio MD, Ychou M, Molina F, Gongora C, Thierry AR (2011) High fragmentation characterizes tumour-derived circulating DNA. PLoS One 6(9):e23418. doi:10.1371/journal.pone.0023418
33. Mouliere F, El Messaoudi S, Gongora C, Guedj AS, Robert B, Rio MD, Molina F, Lamy PJ, Lopez-Crapez E, Mathonnet M, Ychou M, Pezet D, Thierry AR (2013) Circulating cell-free DNA from colorectal cancer patients may reveal high *KRAS* or *BRAF* mutation load. Transl Oncol 6(3):319–328
34. Underhill HR, Kitzman JO, Hellwig S, Welker NC, Daza R, Baker DN, Gligorich KM, Rostomily RC, Bronner MP, Shendure J (2016) Fragment length of circulating tumor DNA. PLoS Genet 12(7):e1006162. doi:10.1371/journal.pgen.1006162
35. Choi J, Reich C, Pisetsky D (2004) Release of DNA from dead and dying lymphocyte and monocyte cell lines in vitro. Scand J Immunol 60:159–166
36. Morozkin ES, Laktionov PP, Rykova EY, Bryzgunova OE, Vlasov VV (2004) Release of nucleic acids by eukaryotic cells in tissue culture. Nucleosides Nucleotides Nucleic Acids 23:927–930
37. Morozkin E, Sil'nikov V, Rykova EY, Vlassov V, Laktionov P (2009) Extracellular DNA in culture of primary and transformed cells, infected and not infected with mycoplasma. Bull Exp Biol Med 147:63–65
38. Sai S, Ichikawa D, Tomita H, Ikoma D, Tani N, Ikoma H, Kikuchi S, Fujiwara H, Ueda Y, Otsuji E (2007) Quantification of plasma cell-free DNA in patients with gastric cancer. Anticancer Res 27:2747–2752
39. Anker P, Stroun M, Maurice PA (1975) Spontaneous release of DNA by human blood lymphocytes as shown in an in vitro system. Cancer Res 35:2375–2382
40. Anker P, Mulcahy H, Chen XQ, Stroun M (1999) Detection of circulating tumor DNA in the blood (plasma/serum) of cancer patients. Cancer Metast Rev 18:65–73
41. Stroun M, Anker P (1972) In vitro synthesis of DNA spontaneously released by bacteria or frog auricles. Biochimie 54:1443–1452
42. Stroun M, Lyautey J, Olson-Sand A, Anker P (2001) About the possible origin and mechanism of cirDNA. Apoptosis and active DNA release. Clin Chim Acta 313(2001):139–142
43. Jahr S, Hentze H, Englisch S, Hardt D, Fackelmayer FO, Hesch RD, Knippers R (2001) DNA fragments in the blood plasma of cancer patients: quantitations and evidence for their origin from apoptotic and necrotic cells. Cancer Res 61:1659–1665
44. Ermakov AV, Konkova MS, Kostyuk SV, Egolina NA, Efremova LV, Veiko NN (2009) Oxidative stress as a significant factor for development of an adaptive response in irradiated and nonirradiated human lymphocytes after inducing the bystander effect by low-dose X-radiation. Mutat Res 669:155–161
45. Ermakov AV, Konkova MS, Kostyuk SV, Smirnova TD, Malinovskaya EM, Efremova LV, Veiko NN (2011) An extracellular DNA mediated bystander effect produced from low dose irradiated endothelial cells. Mutat Res 712:1–10
46. Ermakov AV, Konkova MS, Kostyuk SV, Izevskaya VL, Baranova A, Veiko NN (2013) Oxidized extracellular DNA as a stress signal in human cells. Oxid Med Cell Longev. doi:10.1155/2013/649747
47. Garcia-Olmo D, Garcia-Arranz M, Clemente LV, Gahan PB, Stroun M (2015) Method for blocking tumour growth. Patent US 2015/0071986 A1
48. Puszyk WM, Crea F, Old RW (2009) Unequal representation of different unique genomic DNA sequences in the cell-free plasma DNA of individual donors. Clin Biochem 42(2009):736–738
49. Bronkhorst AJ, Aucamp J, Wentzel JF, Pretorius PJ (2016) Reference gene selection for in vitro cell-free DNA analysis and gene expression profiling. Clin Biochem 49(2016):606–608. doi:10.1016/j.clinbiochem.2016.01.022
50. Gahan PB, Stroun M (2010) The virtosome—a novel cytosolic informative entity and intercellular messenger. Cell Biochem Funct 28:529–538
51. Applied-Biosystems (2015) A complete next-generation sequencing workflow for circulating cell-free DNA isolation and analysis. https://www.thermofisher.com/content/dam/LifeTech/global/life-sciences/DNARNAPurification/Files/cfDNA-app-note-Global-8Pages-FHR.pdf. Accessed 18 Oct 2016
52. Wrzesinski K, Fey SJ (2013) After trypsinisation, 3D spheroids of C3A hepatocytes need 18 days to re-establish similar levels of key physiological functions to those seen in the liver. Toxicol Res 2:123–135
53. Brand M, Nicholls D (2011) Assessing mitochondrial dysfunction in cells. Biochem J 435:297–312
54. Jones W, Bianchi K (2015) Aerobic glycolysis: beyond proliferation. Front Immunol 6:227. doi:10.3389/fimmu.2015.00227
55. Ghesquière B, Wong BW, Kuchnio A, Carmeliet P (2014) Metabolism of stromal and immune cells in health and disease. Nature 511:167–176
56. Diener C, Muñoz-Gonzalez F, Encarnación S, Resendis-Antonio O (2016) Space of enzyme regulation in HeLa cells can be inferred from its intracellular metabolome. Sci Rep 6:28415. doi:10.1038/srep28415